Impurity Effects in Superconductors

Akilan Palanisami

3-10-99

1 Introduction

The physics of superconductors, despite intense research over the past several decades, continues to generate new and unexplained phenomena (in addition to the old, unexplained phenomena). Many of these properties are either caused or can be probed with the use of various impurities. The use of substitutional impurities is, in effect, a method of perturbing the superconductor on the microscopic level, allowing the superconductor to be studied over a wider range of parameters. This make the use of impurities an excellent method with which to check the validity of existing theories (such as BCS) as well as in helping develop new ones (high T_c). This paper focuses on recent research which has yielded unexpected results in both conventional and unconventional superconductivity.

2 Impurities in Conventional Superconductors

Cooper pairs are composed of 2 electrons traveling identical spatial paths, but in time reversed directions. The formation of superconductivity depends on the creation of these Cooper pairs, but what happens in the presence of an impurity? In the case of a magnetic impurity, the impurity moment remains fixed in time. As the exchange interaction between the magnetic impurity and an electron is not time-reversal invariant, it is expected that magnetic impurities would oppose the formation of superconductivity. Non-magnetic impurities have no such effects and one would expect their interaction with Cooper pairs to be much more limited in scope. This behavior was first predicted by Abrikosov and Gor'kov (1) for conventional s-wave superconductors, with the following result (for $\eta \to 0$):

$$T_c/T_{c_0} = 1 - 0.691(\eta/\eta_{cr}) \tag{1}$$

η=impurity concentration
η_{cr}=impurity concentration at which superconductivity destroyed
T_0=critical temperature of doped superconductor
T_{c_0}=critical temperature of undoped superconductor

The majority of magnetically doped conventional superconductors studied follow the above prediction reasonably well for concentrations $\eta < 0.7\eta_{cr}$(2). Above this concentration, departures from the theory are observed(3). This is probably due to the onset of magnetic ordering of the impurity spins(4). Another prediction by Abrikosov and Gor'kov is a decrease of the energy gap with impurity concentration. This can be understood qualitatively as an energy broadening due to the finite lifetime of an impurity spin orientation where:

$$\Gamma \sim h/\tau \tag{2}$$

Γ=energy broadening
τ=impurity spin orientation lifetime

When a sufficient magnetic impurity concentration is reached, the energy gap will no longer correspond to the order parameter and the energy gap will approach zero faster than $T_c(\eta)$. For $\eta > 0.9\eta_{cr}$, the superconductor is gapless, while for $T_c \rightarrow {T_c}^-$, the gap approaches zero for any impurity concentration. These predictions of gapless superconductivity have been verified experimentally with tunneling experiments on PbGd films(5) and specific heat measurements on LaGd(6).

More recent theories have furthered Abrikosov and Gor'kov's original work by going beyond the second order in the exchange constant(7,8) and have included the Kondo effect for J<0(9). These later theories predict the existence of impurity bands within the superconducting energy gap. These bands have been seen experimentally in tunneling experiments (10,11) (see fig. 1).

By calculating phase shifts for conduction electrons scattering off the impurity ions and inserting them into the above theories, Kunz and Ginsburg(12) were able to get good agreement with their tunneling data from InMn alloys. In order to get a good fit, Kunz and Ginsberg noted that the inclusion of partial waves beyond the s-wave (namely p and d wave) are crucial to the calculation.

Direct measurements of the quasi-particle excitations around a magnetic impurity were obtained by Yazdani et al.(13) using scanning tunneling microscopy. Interestingly, excitations were only detected within a few atomic diameters of the impurity, far smaller than the correlation length ξ_0 of $\sim$400 Angstroms(see fig 2). Even more curious is the dependence of the excita-

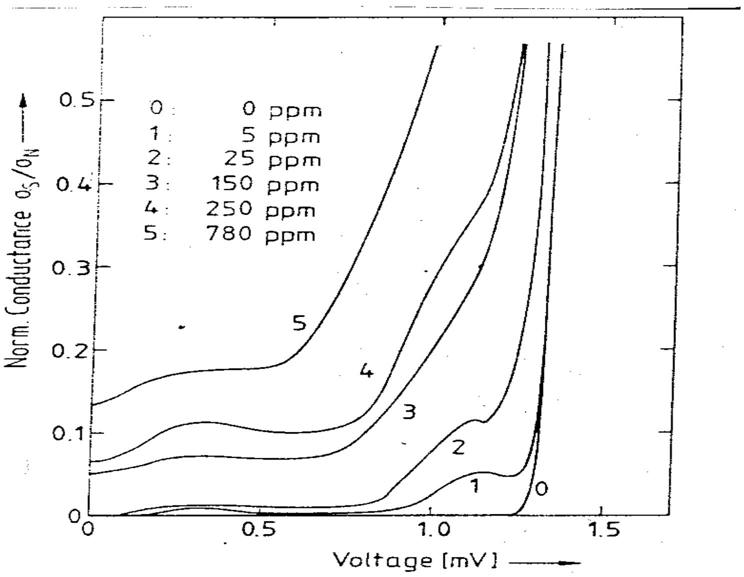

Figure 1: Normalized tunnel conductance for PbMn alloys of different Mn concen. (11)

tions on distance from the impurity. A Mn impurity placed on the surface of niobium created sub-band excitations with a maximum excitation centered directly over the impurity. However, when the impurity is replaced with a single Gd atom, the maximum excitation was measured 6 angstroms away from the impurity. Data taken on ostensibly non-magnetic Ag impurities showed, as expected, no effect on the local density of states. Furthermore, in both cases, the tunneling data was asymmetric with respect to positive and negative bias. Yazdani et al. were able to explain the asymmetry of the data using the Bogoliubov-de Gennes equations, which are coupled Schrodinger-like equations for time-reversed pairs of states in a superconductor (40). In their analysis, the magnetic potential which created the bound state was also found to cause a phase shift in the electron and hole excitation spectrum. For small exchange interaction J, the bound state has a spin aligned to the magnetic impurity and electron like excitations are slightly favored over hole like excitations. Increasing J results in an increase of the phase shift between the electron and hole excitation spectrum as well as the motion of the bound state away from the edge of the gap towards the center (E_F). At a critical

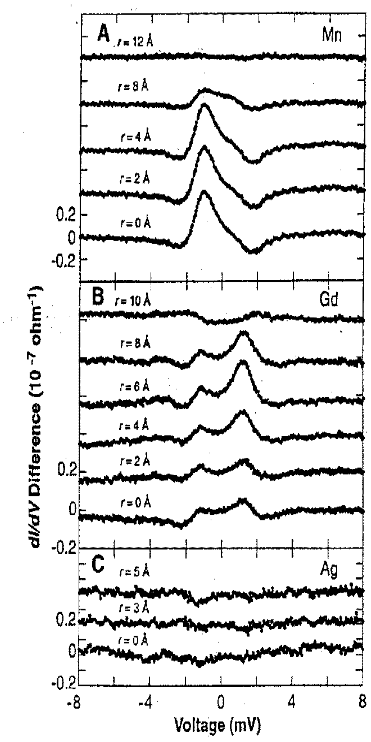

Figure 2: The difference spectra measured near (A) Mn, (B) Gd, and (C) Ag adatoms. The presence of peaks in the data indicates the presence of excitations within Nb's energy gap near the magnetic impurity. The data measured at different distances are offset for clarity. The backround used in each case was measured with the tip over the bare Nb surface 30 angstroms away.(13)

value of J, the phase shift goes to $\pi/2$ and the bound state is on E_F. Above the critical J, the bound excitation moves back towards the edge of the gap and the asymmetry between the hole and electron excitations switch, with the holes now being favored on the impurity site. Looking at the figure, it can be seen Mn qualifies as a strong magnetic impurity, which is reasonable due to the strong magnetic overlap of the d orbitals. This model was unable to explain the spectrum about the Gd impurity.

3 Impurities in non-BCS superconductors

The effects discussed thus far were for BCS s-wave superconductors, but other impure superconductors display properties which are contrary to the above description. In d or p-wave pairing, it is expected that the phase of the superconducting gap function change sign around the Fermi surface. This sign change makes the superconductor much more sensitive to non-magnetic defects, as scattering off of these defects is now a source of pair breaking. This results in a lowering of T_c. In s-wave pairing, the phase does not change sign, although the gap may change in magnitude if the Fermi surface is anisotropic. In this case, scattering off of non-magnetic impurities will also reduce T_c, but not by as much since the scattering will serve only to average out the anisotropy. By noticing these different effects of impurity doping on pairing symmetries, the information can be gleaned about the nature of the pairing mechanism on the microscopic level. However, the results from such measurements, though suggestive, are often not completely conclusive and often raise more questions.

3.1 Impurities Effects in Sr_2RuO_4

One such example of non-magnetic impurities suppressing superconductivity at low concentrations is Sr_2RuO_4(15). In this system, concentrations of 50-100 ppm of Al and Si are seen to strongly suppress superconductivity (see fig. 3). In many cuprates, it has been noted that nominally non-magnetic impurities induce magnetic moments when in a bulk superconductor (see next section). In order to ensure these impurities were, in fact, having no magnetic effect on the system, SQUID magnetometry measurements were taken on the system, and no evidence of magnetic moments were found. In order

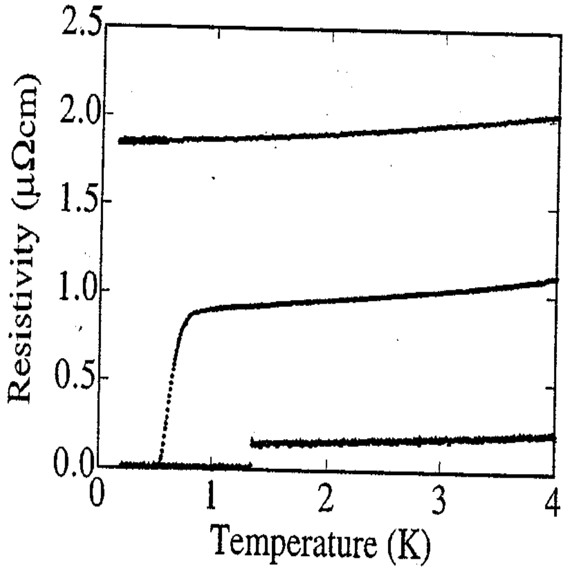

Figure 3: The temperature dependence of the resistivity of between 130 mK and 4K of three single crystals of Sr_2RuO_4 with impurity concen. of ∼400 ppm Al, 50 - 100 ppm Al and some Si (∼ 100ppm), and ∼100 ppm Si in order of decreasing resistivity(15).

to explain the effects of these non-magnetic impurities, a generalization of the Abrikosov-Gor'kov theory for magnetic impurities in a conventional superconductor to non-magnetic impurities in an unconventional superconductor(16) was used. This theory finds that below a critical mean free electron path, superconductivity is completely suppressed, which is in agreement with the data and suggests Sr_2RuO_4 has unconventional pairing, as superconductivity would not be completely suppressed in an s-wave superconductor as mentioned previously. Other impurities were also noted in the experiment (such as Bi), but found to have less of an effect as they resided off the oxygen planes which are known to play a dominant role in the conduction.

3.2 Impurity Effects in $YBa_2Cu_3O_{7-\delta}$

A lot of work has been done in impurities in $YBa_2Cu_3O_{7-\delta}$. In particular, Ni and Zn impurities are commonly used as they are known to replace Cu on the copper oxide planes(17,19). Zn is an interesting case, as valence counting suggests a Zn impurity with the same charge as the displaced copper atom (Cu^{2+}) would have a $3d^{10}$, S=0 valence state, resulting in no magnetic moment. However, Zn is known to be much more effective in suppressing superconductivity than Ni(18). For instance, in the superconducting state, Zn is seen to be 2-3 times more effective at lowering T_c. In addition, the electromagnetic properties of the superconductor are strongly altered. In clean $YBa_2Cu_3O_{7-\delta}$, the penetration depth is found to vary linearly with temperature, but as little as 0.15% Zn impurity distorts the linear behavior, and 0.31% Zn impurity gives rise to quadratic behavior, which is indicative of gapless superconductivity. Meanwhile, concentrations of 0.75% Ni are seen to have very little effect on the temperature dependent penetration depth(20) (see fig. 4). One explanation lies in the fact that Ni acts as a Born scatterer, while Zn behaves as a resonant scattering site. Another posited explanation suggests Zn impurities alter the local spin fluctuations on the copper oxide planes (21). NMR and magnetization measurements in the normal state have suggested that Zn induces a weak magnetic moment of approximately 0.32-0.36 μ_B/Zn for fully oxygenated crystals, and that this moment increases as the oxygen content decreases (18,22). Similar measurements have shown Ni to have a moment of $1.5\mu_B$ (S=1/2)(18), illustrating that the strength of the moment is not the sole determining factor in the suppression of superconductivity.

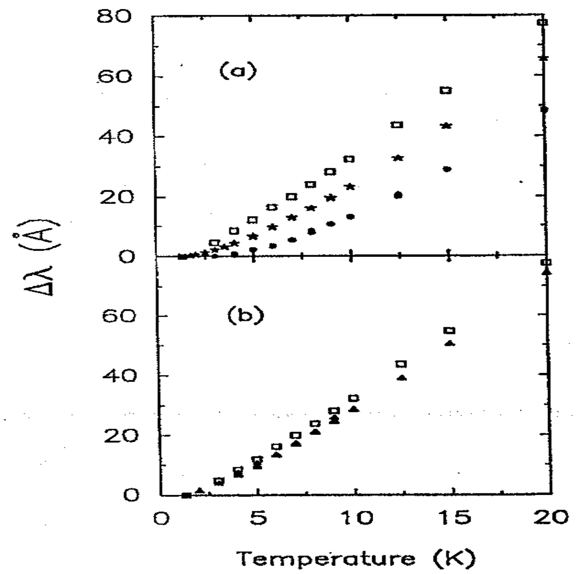

Figure 4: Comparison of the effect of (a)Zn and (b)Ni impurities on the temperature dependence of the London penetration depth. The sequence shown in (a) from pure (squares), 0.15% (stars), 0.31%(solid circles) substitution of Zn for Cu shows a change from linear temperature dependence to quadratic. (b) shows that 0.75% substitution of Ni impurities (solid triangles) has little effect on the penetration depth.(20)

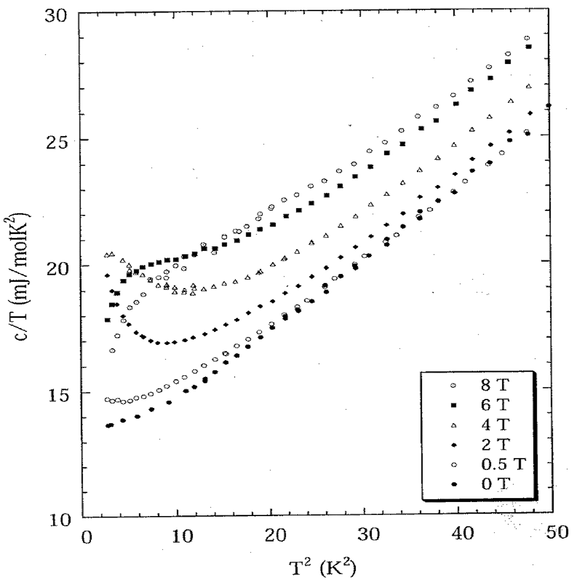

Figure 5: Temperature dependence of the specific heat (plotted as c(T)/T of 1% Zn doped $YBa_2Cu_3O_{7-\delta}$, cooled in applied fields from 0 to 8 tesla (23)

A more recent specific heat measurement(23), performed in a magnetic field on polycrystalline $YBa_2Cu_3O_{6.97}$ found a number of interesting changes in the specific heat curve as the Zn impurity concentration increased. Firstly, it was noted that the T^3 term of the specific heat decreases as Zn concentration increases, suggesting either an increase in the Debye temperature or a new electronic contribution to the specific heat. If this increase is due entirely to the lattice contribution, the change corresponds to a Debye temperature of 403K for pure $YBa_2Cu_3O_{6.97}$, as compared to 454K for a 1% Zn doped sample. Such a large increase is unusual and may indicated that part of the T^3 is electronic in nature. Secondly, the linear temperature term (the electronic contribution) of the specific heat at zero magnetic field was noted to increase with Zn concentration. This increase can be interpreted as an increase in the residual density of states. For low Zn concentrations (less than 1%), this increase matches well with penetration depth data interpreted using a "dirty d-wave" analysis(26). Thirdly, a low temperature upturn (T^{-2}) below $\sim$3.5K is also seen in the Zn doped $YBa_2Cu_3O_{7-\delta}$ (see fig. 5). The exact origin of this term is unknown, but it may be due to interactions of the paramagnetic impurities with the local field or a collective interaction of the impurities(27). The fact that the upturn depends on the quality of the sample lends some support to these explanations.

Finally, the most interesting result of all stems from the expectation of the magnetic field splitting the Zn-induced magnetic moments into a two level system, introducing a Schottky anomaly into the specific heat. Surprising, no such feature is observed. To make this observation, it must first be noted that a Schottky anomaly is always found in specific heat measurements of pure $YBa_2Cu_3O_{6.97}$. For optimally doped $YBa_2Cu_3O_{6.97}$, a molar concentration of 0.05-0.1% spins per copper atom is measured(28). For higher oxygen concentrations, the number of spins is smaller, indicating that the moments arise from uncompensated copper atoms in the chain. Taking this addition Schottky anomaly into account, an upper limit of 0.02% (molar concentration) spins per copper atoms was measured for 1% Zn doping. Sisson et al. give two explanations. The first is that the moments exist only locally and will therefore not be found in bulk measurements (like the specific heat) but can be detected only through local measurements, such as the Knight shift(29). The second explanation uses a screening similar to Kondo screening(30). In conventional superconductors, Abrikosov and Gor'kov showed that the Kondo effect is suppressed by the formation of the superconducting gap. In a d-wave superconductor, it is theorized that magnetic impurities will be screened by the node lines in the superconducting gap. This latter theory has been fit to the data with good results.

3.3 Impurity Effects in $YBa_2Cu_4O_8$

Investigations in impurity doped $YBa_2Cu_4O_8$ provide a nice contrast to $YBa_2Cu_3O_{7-\delta}$ as the oxygen content in the latter can vary with δ ranging from 0 to 1. This variability can cause confusion of the effects due to impurities and changes in oxygen content. In addition, oxygen disorder leads to broadening of the ^{89}Y NMR resonance. There are no such troubles with $YBa_2Cu_4O_8$ as its oxygen content is constant.

$YBa_2Cu_4O_8$ displays properties substantially different from $YBa_2Cu_3O_{7-\delta}$. Both $YBa_2(Cu_{1-x}Zn_x)_4O_8$ and $YBa_2(Cu_{1-x}Ni_x)_4O_8$ show a similar decrease of T_c with impurity concentration, with T_x=0 when c(=$4x$)$\sim$0.12 (31), as opposed to $YBa_2Cu_3O_{7-\delta}$, where Zn and Ni have very different effects. Thermopower data(34) of doped $YBa_2Cu_4O_8$ has shown that the decrease

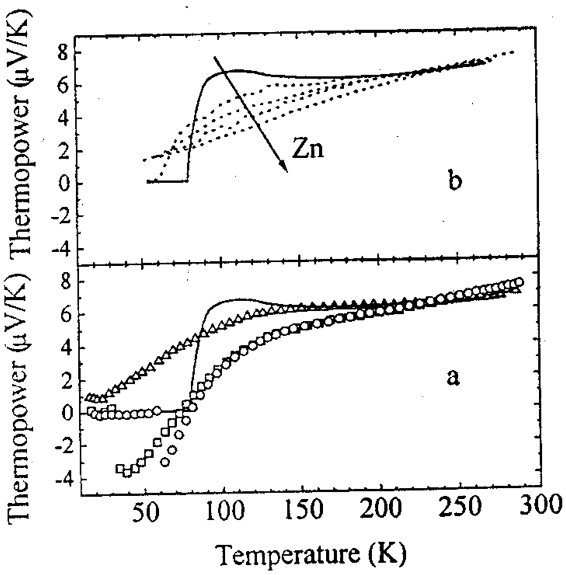

Figure 6: Plot of thermopower against temperature for (a) $YBa_2(Cu_{1-x}Ni_x)_4O_8$ with (solid line) x=0, (circle) x=0.0125, (square) x=0.025, and (triangle) x=0.05; (b)Plot of thermopower against temperature for $YBa_2(Cu_{1-x}Ni_x)_4O_8$ with x=0, 0.00625, 0.0125, 0.025, 0.0375 (34)

in T_c cannot be attributed to a lack of holes. This can be seen in figure 6 (to interpret this data properly, one must note that the room temperature thermopower of the high-T_c cuprates varies systematically with hole concentration). Therefore a constant room temperature thermopower for different impurity concentrations implies a constant hole concentration. NMR and thermopower (32) studies have shown the energy gap in $YBa_2(Cu_{1-x}Zn_x)_4O_8$ to be locally suppressed around the Zn impurity. Away from the impurity, it is found that, for low concentrations, the gap begins to fill in, but E_g stays relatively constant. This behavior has been attributed to a Zn induced magnetic moment (like in $YBa_2Cu_3O_{7-\delta}$)(33). The fanning out of the thermopower data in fig. 6 below 220K can be attributed to this distortion of the energy gap near Zn, but remaining unchanged far away.

Similar NMR studies of Ni doped $YBa_2Cu_4O_8$ show no such distortion of the energy gap anywhere near the Ni impurity. Thermopower measure-

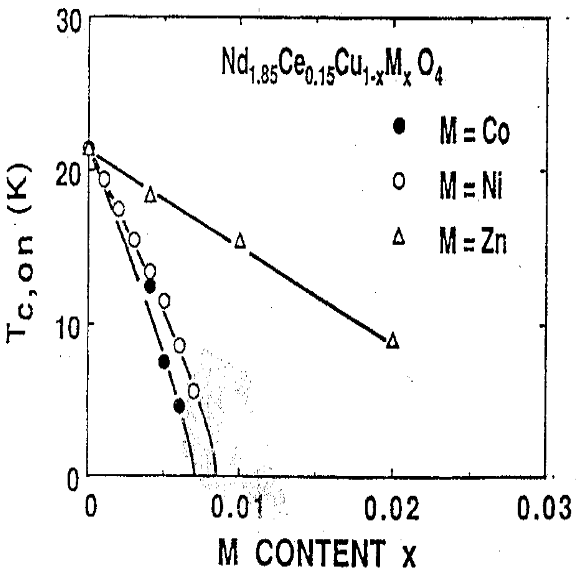

Figure 7: The relationship between T_c and dopent concen. x for $Nd_{1.85}Ce_{0.15}Cu_{1-x}M_xO_4$(35)

ments of Ni doped $YBa_2Cu_4O_8$ also display some perplexing features. The low temperature thermopower is seen to be negative for particular impurity concentrations. Perhaps related to this is the increase in thermopower at higher Ni concentrations. Neither of these features have been explained.

3.4 Impurity Effects in Electron Doped Superconductors

Electron doped superconductors, as opposed to the hole doped superconducting cuprates, appear to be much more sensitive to impurities. 0.7% Co and 0.8% Ni substitution for Cu in $Nd_{1.85}Ce_{0.15}CuO_4$ has been seen to completely suppress superconductivity. While T_c is observed to decrease linearly with respect to Zn impurity concentration, with T_c ~9K for a Zn concentration of 2%(35)(see fig. 7). This is completely opposite what is seen with $YBa_2Cu_3O_{7-\delta}$. Furthermore, the T_c versus impurity concentration for Co and Ni were found to match well with Abrikosov and Gorkov's theory for paramagnetic impurities, suggesting the pair breaking mechanism

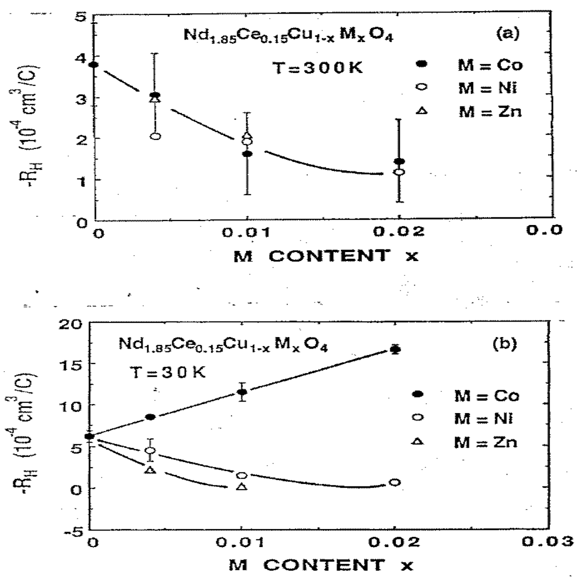

Figure 8: The relationship between Hall coefficient and dopent concen. x for $Nd_{1.85}Ce_{0.15}Cu_{1-x}M_xO_4$ (a) at 300K, (b) at 30K.(35)

discussed before. Studies done on $La_{1.85}Sr_{0.15}CuO_4$ (a p-type superconductor)(36,37,38) showed that more than more than 5% Co, 5% Ni, and 2.2% Zn were required to destroy superconductivity. These numbers are considerably larger than those measured for $Nd_{1.85}Ce_{0.15}CuO_4$, but the crystal structures are quite similar. If pair breaking is the dominant mechanism, the exchange interaction energy between an electron and a paramagnetic impurity in an n-type superconductor should be much larger than that of a hole and a paramagnetic impurity in a p-type superconductor. Conclusive results for this prediction were not found in the literature. Looking at Hall coefficient (R_H) data (see fig. 8), it can be seen at 300K, $|R_H|$ decreases monotonically for all 3 impurities and the rate of decrease is practically independent of the impurity species. This indicates that all 3 species are in a divalent state at 300K and are not affecting the charge balance in the CuO_2 planes. At 30K however, the $|R_H|$ of the Co doped sample increases proportionally with doping, while the Zn and Ni doped samples decrease monotonically with doping. One possible interpretation of the Co doped sample's deviation is a phase transition from the S=3/2 state to the S=1/2 state of the Co^{2+} ion(39). Detection of such a change in Co^{2+} spin is complicated by the large magnetic moment of the Nd^{3+} ions.

No clear relationship was apparent between T_c and the variations in R_H. However, looking at dp_H/dT, where p_H is the normalized Hall density defined here as follows:

$$p_H = n_H \frac{V}{N} = |\frac{1}{R_H e}| \frac{V}{N} \tag{3}$$

n_H=conventional Hall density
e=elementary electron charge
V=unit cell volume
N=number of Cu ions per unit cell

It was found that dp_H/dT increased with increasing impurity concentration, and hence had a negative correlation with T_c.

4 Conclusion

Although many of the effects of impurities have been predicted by Abrikosov and Gor'kov and extensions, there are many properties of impurity doped superconductors which are not easily understood. This is especially true of unconventional superconductors, where the relative strengths of magnetic and non-magnetic impurities are specific to the superconducting host. This paper has given just a brief sampling of the experimental efforts directed towards impurity effects and has barely mentioned the efforts of theorists in this field. Completely neglected here was the role of impurities in type II superconductors as vortex pinning sites. I mention these topics in passing as they are vast fields on their own and were too large to include here.

5 References

(1) A.A. Abrikosov, L.P. Gor'kov, Sov. Phys. JETP 12, 1243 (1961)
(2) M.B. Maple in Magnetism, H. Suhl, Ed. vol. V, pp 289-325
(3) R.A. Hein, R.L. Falge Jr., G.T. Matthias, E. Corenzwit, Phys. Rev. Lett. 2, 500 (1969)
(4) K.H. Benneman, ibid. 17, 438 (1966)
(5) M.A. Woolf, F. Reif, Phys. Rev. A. 137, 557 (1965)
(6) D.K. Finnemore, D.L. Johnson, J.E. Ostenson, F.H. Spedding, B.J. Beaudry, ibid. 137, 550 (1965)
(7) H. Shiba, Prog. Theor. Phys. 40, 435 (1968)
(8) A.I. Rusinov, Sov. Phys. JETP 29,1101 (1969)
(9) J. Zittartz, A. Bringer, E. Muller-Hartmann, Solid State Comm. 20, 513 (1972)
(10) J.K. Tsang, D.M. Ginsberg, Phys. Rev. B. 21, 132 (1980)
(11) W. Bauriedl, P. Ziemann, and W. Buckel, Phys. Rev. Lett. 47, 1163 (1981)
(12) A.B. Kunz, D.M. Ginsberg, Phys. Rev. B. 22, 3165 (1980)
(13) A. Yazdani, B.A. Jones, C.P. Lutz, M.F. Crommie, D.M. Eigler, Science 275, 1767 (1997)
(14) W. Chung, M. Jarrell, Phys. Rev. Lett. 77, 3621 (1996)
(15) A.P. Mackenzie, R.K.W. Haselwimmer, A.W. Tyler, G.G. Lonzarich, Y. Mori, S. Nishizaki, Y. Maeno, Phys. Rev. Lett. 80, 161 (1998)
(16) R.J. Radtke et al., Phys. Rev. B 48, 653 (1993)
(17) G.Xiao et al., Nature(London) 332, 238 (1988)
(18) P. Mendels, H.Alloul, G. Collin, N. Blanchard, J.F. Marucco, J. Bobroff, Physica C 235-40, 1595 (1994)
(19) H. Maeda et al., Physica C 157, 483 (1989)
(20) D.A. Bonn, S. Kamal, K. Zhang, R. Liang, D.J. Baar, E. Klein, W.N. Hardy, Phys. Rev. B. 50, 4051 (1994)
(21) P. Monthoux, D. Pines, ibid. 49, 4261 (1994)
(22) S. Zagoulaev, P. Monod, J. Jegoudez, ibid. 52, 10474
(23) D.L. Sisson, S.G. Doettinger, A. Kapitulnik, R. Liang, D.A. Bonn, W.M. Hardy, Los Alamos Preprint Archive (xxx.lanl.gov) cond-mat/9904131, 9 Apr. (1999)
(24) K. Ishida, Y. Kitaoka, N. Ogata, T. Kamino, K. Asayama, J.R. Cooper, N. Athanassopoulou, J. Phys. Soc. Jpn. 62, 2803 (1993)

(25) J.W. Loram, K.A. Mizra, P.F. Freeman, Physica C171, 243 (1990)
(26) P.J. Hirschfeld, W.O. Putikka, D.J. Salapino, Phys. Rev. B 50, 10250 (1994)
(27) J.S. Urvack, D.B. Mitzi, A. Kapitulnik, J.Y.T. Wei, D.E. Morris, ibid. 39, 12391 (1989)
(28) K.A. Moler, D.L. Sisson, J.S. Urbach, M.R. Beasley, A. Kapitulnik, D.J. Vaar, R. Liang, W.N. Hardy, ibid 55, 3954 (1997)
(29) A.W. Sandwik, E. Dagotto, D.J. Scalapino, ibid. 56, 11701 (1997)
(30) C.R. Cassanello, E. Fradkin, ibid. 56, 11246 (1997)
(31) N. Watanabe, N. Koshizuka, N. Seiji, H. Yamauchi, Physica C 234, 361 (1994)
(32) G.V.M. Williams, J.L. Tallon, R. Meinhold, A. Hanossy, Phys. Rev. B. 51, 16503 (1995)
(33) G.V.M. Williams, J.L. Tallon, R. Meinhold, ibid. 52, R7034 (1995)
(34) G.V.M. Williams, J.L. Tallon, R. Dupree, R. Michalak, Phys. Rev. B. 54, 9532 (1996)
(35) J. Sugiyama, S. Tokuono, S. Koriuama, H. Yamauchi, S. Tanaka, ibid. 43, 10489 (1991)
(36) G. Xiao, A. Bakshia, M.Z. CIeplak, Z. Tesanovic, and C.L. Chien, ibid 39, 315 (1989)
(37) W. Wang, H.J. Schulz, K. Jerome, S.S.P. Parkin, J.M. Bassat, Ph. Odier, ibid. 37, 5132 (1988)
(38) J.M. Tarascon, E. Wang, S. Kivelson, B.G. Bagley, G.W. Hull, R. Ramesh, Ivid. 42, 218 (1990)
(39) L.R. Le Coustumer, Y. Barbaux, J.P. Bonnelle, Nuov. J. Chem. 6, 7 (1982)
(40) P.G. de Gennes, Superconductivity in Metals and Alloys (Addison-Wesley, Reading, MA, 1989